



Experimental and Numerical Studies of Two-Phase Flow in Ribbed Periodic Vertical Channel

Open
Access

Laith Jaafer Habeeb^{1,*}, Hasan Shakir Majidi²

¹ Training and Workshop Centre, University of Technology, Baghdad, Iraq

² Department of Chemical and Petroleum Industries Engineering, Al-Mustaqbal University College, Iraq

ARTICLE INFO

ABSTRACT

Article history:

Received 13 October 2019

Received in revised form 30 December 2019

Accepted 31 December 2019

Available online 25 March 2020

Pressure drop in a ribbed vertical channel was studied for a two-phase (air and water) flow, different shapes of ribs (triangle, semi-circular, and rectangle) were used in this investigation. An experimental rig was constructed with a test channel having the dimensions (10×3×70 cm) that enabled the flow patterns visual observation. An experimental setup of a two-phase was done for the present investigation, as well as a sum of (150) two-phase data with various flow patterns was determined. The used water superficial inlet velocities were in the range (0.0333 - 0.0888 m/s), and the air superficial inlet velocities were in the range (0.0555 - 0.1666 m/s). The experimental pressure drop according to a smooth plate was (41%, 38%, and 35%) for a channel fitted with semi-circle, rectangular and triangular ribs, respectively. The less pressure drop recorded was in the triangular ribbed channel, which indicates that the triangular shaped ribbed channel is the finest shape among the studied ones to lower the pressure drop. As future work, the numbers and dimensions of ribs can be changed to investigate its effect on the two-phase flow and the pressure drop, another suggestion for the future investigations is to include other fluid to have a three-phase flow, also the inclination angle of the duct can be changed to study its effect.

Keywords:

Two-phase flow; Semi-Circular ribs;
Rectangular ribs; Triangular ribs; CFD

Copyright © 2020 PENERBIT AKADEMIA BARU - All rights reserved

1. Introduction

The periodic ribs are frequently used in the heat exchanger design and the other passages for cooling. Since the flow around the ribs include the recirculation, reattachment and secondary flow, and the detailed temperature, Weisman *et al.*, [1] performed a set of experimental tests on double and single ribbed helical tubes with circular cross section; two-phase flow was used for the experiments. The pressure drop and the flow pattern were investigated. They found that when the minimum velocity of liquid was exceeded for low qualities an annular swirling flow could be seen. They devised a dimensionless correlations for the observed transitions in the flow pattern. The

* Corresponding author.

E-mail address: laithhabeeb1974@gmail.com (Laith Jaafer Habeeb)

research on the ribs for increase the heat transfer in pipes are diverse however, the investigations on their effect on the pressure drop are not so many, Gao and Sundén [2]. Asano *et al.*, [3] experimentally investigated the adiabatic two phases flow (air-water) and the (R141b) boiling two phases flow in the heat exchangers having an individual channel positioned in a vertical direction. For the boiling two-phase flows, the spreads of liquid in test section were influenced via the states (the liquid stagnation at the test section inlet and inlet flow pattern.). Thus, the distributions of liquid were too distinct if the working fluids were moved through the test section like a single-phase or two phases flow. Ansari and Arzandi [4] studied experimentally two phases (air-water) flow utilizing rectangular ducts, which are having a smooth surface and ribbed for depicting the ribs height influence upon the boundaries, and the authors introduced a flow map diagram. Three ribs were used; it was found that the increasing of rib height initiated a hydro-dynamical instability at lower fluid velocities. Habeeb and Al-Turaihi [5] investigated the two-phase (air-water) flow around a triangular-section obstacle in a rectangular channel experimentally and numerically for steady and unsteady flows. The horizontal rectangular channel was made of transparent Perspex with (3.175 cm) outer diameter. The flow behavior and pressure difference were studied. Four different values of water flow rate (20, 25, 35, 45 l/min), also (4) different values (10, 20, 30 and 40) l/min of the flow rate of air were used. CFD was used to perform a numerical study by fluent package. It was found that the pressure difference increased as the flow rates of air or water were increased, and more turbulence was seen which produced more bubbles and waves. Jiang G. *et al.*, [6] studied experimentally and numerically the characteristics of the flow and heat transfer of a (mist/steam) two phases flow in an elevated temperature square channel with ribs of (60°). Firstly, a 3D coupled numerical model of fluid-solid was set to this channel cooled via the (mist/steam). The numerical outcomes well agree with the experimental ones, and the ultimate deviation of temperature of the centerline of the lower wall is lower than 4.6%. After that, the longitudinal vortex influence, “mainstream affected region” spread, and “vortex affected region” upon the temperature spread of the channel wall were qualitatively analyzed in accordance with the outcomes of the simulation. Eventually, the key parameters effect, which are the mass ratio of (mist/steam), heat flux, and the diameter of the water droplet diameter as well as the Re number upon the characteristics of transfer of heat and flow were investigated employing such numerical approach. These conclusions can be attained: if the (Re) raises within a range of (74,000-170,000), the average centerline Nu no. increases within a range of (376.3-882.2), under state (mist/steam = 3%) and ($q = 8000 \text{ Wm}^{-2}$). When the mass ratio of the mist/steam rises within a range of (0.5-9%), the average Nu no. increases within a range of (636.3-996.3) under inlet state ($q = 8000 \text{ Wm}^{-2}$) and (Re=147,000). The (f/f_1) ratio raised about (22%) if the Re increases within a range (74,000-170,000) under state ($q = 8000 \text{ Wm}^{-2}$). The mass ratio of the mist/steam possesses a slight effect on the ($f=f_1$); and the ($f=f_1$) ratio is raised slowly with heat flux. If the mist/steam ratio and the heat flux are sure, the heat transfer enhancement raises via friction resistance rising. Parsaiemehr *et al.*, [7] numerically simulated the Water/ Al_2O_3 nanofluid heat transfer and the turbulent flow in a rectangular channel, the main purpose for the study was to investigate the influence of the angle of attack of a rib having an inclined rectangular shape, nanoparticles volume fraction, and the (Re) no. on the heat transfer enhancement. Owing to such reason, the turbulent flow of a nanofluid was simulated for (Re) nos. in the range (15000-30000) as well as for the nanoparticles volume fractions in the range (0-4%). Variations of the ribs angle of attack were studied over the range (0- 180°). Outcomes showed that the ribs angle of attack variations owing to the variations of the flow pattern in addition to the generated vortices in channel possess an important influence upon the fluid blending. In addition, the ultimate rate of the enhancement of heat transfer completes in the (60°) attack angle. In (Re) nos. of (15000), (20000) and (30000) and (60°) attack angle, in comparison with the (0°) attack angle, the Nusselt no. amount improved by

(2.37, 1.96 and 2) times, correspondingly. In addition, it was inferred that at high (Re) nos., via utilizing nanofluid and ribs, the performance evaluation criterion improves. Jiang *et al.*, [8] studied numerically the heat and flow characteristics a (mist/steam) two phases flow inside a turbine blade's internal passage for cooling and having a "U" shape. The quality (k- ϵ) model was utilized, because the model of turbulence united with the model of (DPM) for calculating the (mist/steam) mass quantitative relation effect as well as the mist diameter upon the flow and the warmest transfer of the U-shaped flow U-shaped U-passage with totally various formed ribs. The outcome indicated that below the fixed working state, the U-shaped channel having (45°) formed ribs possesses a higher performance of heat transfer than various channels, also the warmth transfer heterogeneity of the channel with a "U" shape and having ribs of 75° is the worst case among the whole channels investigated through the present work. The performance of warmth transfer of the channel having a "U" shape and formed ribs is greater than the channel with paralleled ribs. For the cooling of mist/steam within the U-shaped passage with the similar structure of ribs, the heterogeneity of heat transfer raises with the rising of the performance of warmth transfer. Once the diameter of mists raises from (5 μm) to (15 μm), the performance of warmth transfer of the "Second-Flow-Passage" will increase clearly, and the heat transfer heterogeneity rises instantaneously. The performance of warmth transfer has not increased once the diameter of mists unceasingly increases and it is larger than 10 μm . Shi *et al.*, [9] studied the characteristics of the heat transfer and flow of the (mist/steam) coolant inside a gas turbine cooling passage having "U" shape. The mass ratio of (mist/steam) and the mist diameter are cautiously analyzed via a numerical approach; outcomes showed that the ribbed-wall heat transfer rises gradually with increasing the mass ratio of the (mist/steam). At the case of 10 μm diameter of water mist, as the mass ratio of mist rises within the range (2-10%), the averaged (Nu) no. of the "First-Flow-Passage" rose up to 60.13%, and the "Second-Flow-Passage" rose up to 112.5%. The mist evaporation rate and the surviving time are governed via governing the diameter of mists. The big diameter of mist diameter isn't usually adequate to enhance the ribbed walls heat transfer. If the mist/steam is (8%), like for the "First-Flow-Passage" and the "Second-Flow-Passage", the (10 μm) diameter water mists possess a greater average Nu no. of the ribbed wall than the (5 μm , 15 μm and 20 μm) mists. The enhancement of the performance of heat transfer resulted from the water mist evaporation is limited to increasing the heterogeneity of the heated walls heat transfer. Ayagara *et al.*, [10] used numerical and experimental approaches to study the dynamic behavior characterization for ribs that were porcine isolated. They used bending tests with three-point setup of Split Hopkinson Pressure Bar, the results of the fracture patterns and the force displacement curves were highly predicted using the finite element model. Park *et al.*, [11] performed a number of experiments to investigate the pressure gradients for two phase (water-air) flow, under conditions that were isothermal. For low superficial air velocity, the dimensionless pressure gradients decrease rapidly, which is due to the reduction of the hydrostatic head due to an increase in the void fraction as the superficial air velocity increases. Wang *et al.*, [12] experimentally studied the two-phase flow regimes at high pressure horizontal pipe. They reached a good performance for model of regime transition. Seven flow regimes were obtained, such as smooth stratified flow, wave stratified flow, annular flow, annular mist flow, slug flow, plug flow and bubble flow. With pressure increased, density of gas phase is significantly increased by nearly 20 times. Jawad *et al.*, [13] studied the performance prediction of a modified centrifugal compressor used in turbo charger numerically. The researchers aimed to study and simulate the effect of impeller trimming on the performance of a turbocharger compressor. It was observed the performance was greatly affected by the double splitter design and the pressure ratio and air mass flow rate were increased.

The characteristics of the flow field of two-phase (air/water) flow in a rectangular duct with three different rib shapes were studied in this paper experimentally and numerically using ANSYS Fluent software as previous studies did not deal with it. Different shapes of ribs were used for this investigation. The results from the different ribs shapes were compared to find the acceptable ribs shape with the acceptable flow characteristics.

2. Experimental Setup

A model Rectangular channel is made to study the effect of water and air superficial velocities on the flow pattern and the pressure drop, also to show the influence of the ribs shape on pressure drop. Figure 1 shows a schematic diagram for the experimental rig used in this work. The equipment used to build the experimental rig consists of a pump joined with a flowmeter. This pump is from Hitachi Ltd. type (ov) [14], and it has 8 m head and $0.08 \text{ m}^3\text{min}^{-1}$ specification quantity. The flowmeter has a range of ($10\text{-}80 \text{ L}\cdot\text{min}^{-1}$) volume flow rate. The air compressor was utilized for supplying the air (phase of gas). A compressor kind is Recommend Amos Aceite-Worthington [15]. It possesses 0.5 m^3 capacity and 16 bar peak pressure. Air flowmeter was employed for measuring the rate of airflow that goes through the channel, DK800 glass tube flowmeter [16], and it possesses a range of ($5.833\text{-}58.33 \text{ L}\cdot\text{min}^{-1}$) flow rate. The test section possesses a ($8 \text{ cm}\times 3 \text{ cm}$) rectangular cross section and 70 cm length, for steadying the behavior of two phases flow (air and liquid) around the whole ribs. Four Pressure sensors were used to read the pressure of the test pipe with a range of (0-1bar), the accuracy of these sensors is (0.1%). A "Sony digital video camera recorder", model "DCR-SR68E" [17], with 80 GB capacity and having "Carl Zeiss Vario-Tessar" lens of 60x (optical) and 2000x (digital) was utilized for visualizing the flow structures. Experiments were conducted for showing the influence of various working circumstances upon the difference of pressure a cross the section of test. These circumstances are discharge of water and discharge of air. The experimental rig used for the test and the measuring system are shown in Figure 2. Perspex transparent channel was used with ($10 \text{ cm}\times 3 \text{ cm}$) rectangular cross section and (70 cm) length with a pipe of water having a diameter of (3.175 cm). Three various ribs shapes were investigated which are (triangular, semi-circle, and rectangular), as depicted in the Figure 3, a smooth channel was also created for showing the difference produced via the ribs. These ribs possess a height of ($d=0.6 \text{ cm}$) and a base width of ($p = 1.2 \text{ cm}$) along with ($w = 0.5 \text{ cm}$) pitch distance. Ribs are placed and fastened via a screw and nut on a blind panel on the rectangular channel left side at (5.0 cm) from the test section entrance. Water was pumped with a (500 L/min) peak discharge from the tank of water and exerted into the section of test. A Flowmeter was utilized for measuring the water volume flow rate within a range of ($0\text{-}30 \text{ L}\cdot\text{min}^{-1}$). An air compressor having a 0.5 m^3 capacity and 16 bar peak pressure was employed to provide the gas phase (air) into the test section. Air flowmeter of range ($5.833 \text{ L}/\text{min}$ to $58.33 \text{ L}/\text{min}$) was employed for measuring and controlling the air volume flow rate. The camera has a high accuracy of ($\pm 2^\circ\text{C}$) or ($\pm 2\%$) and a frame rate of 9 HZ. The phase of air and the phase of water were blended in a blending apparatus prior entering the channel. Table 1 shows the dimensions of the ribs used.

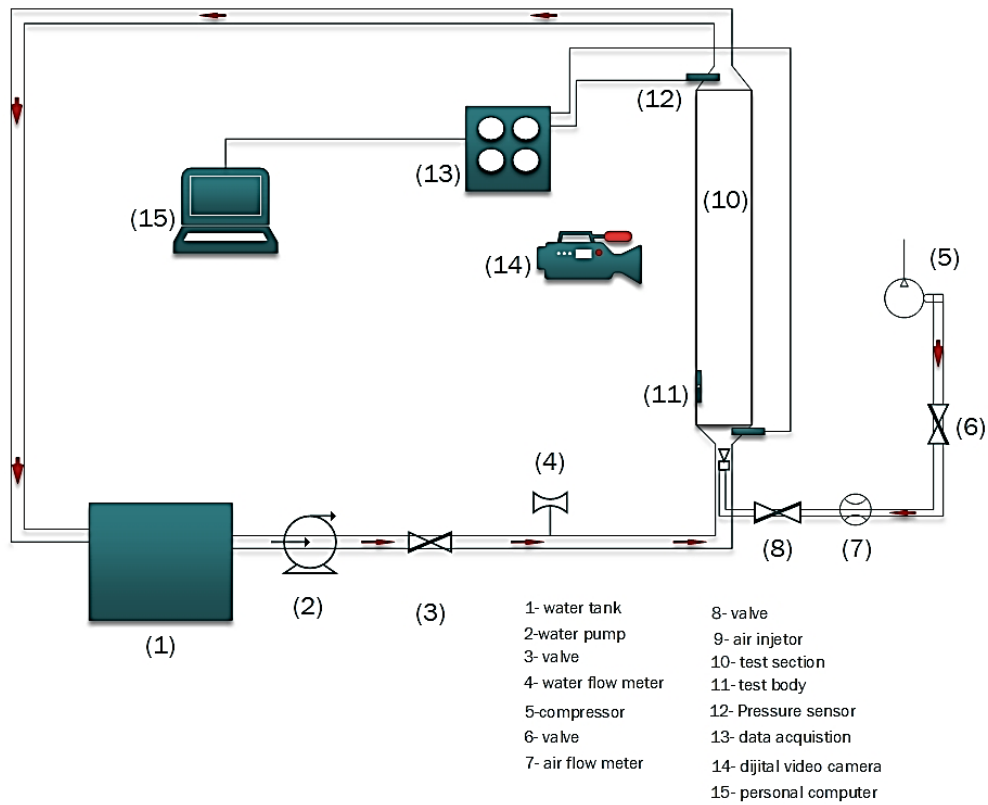


Fig. 1. The test rig diagram

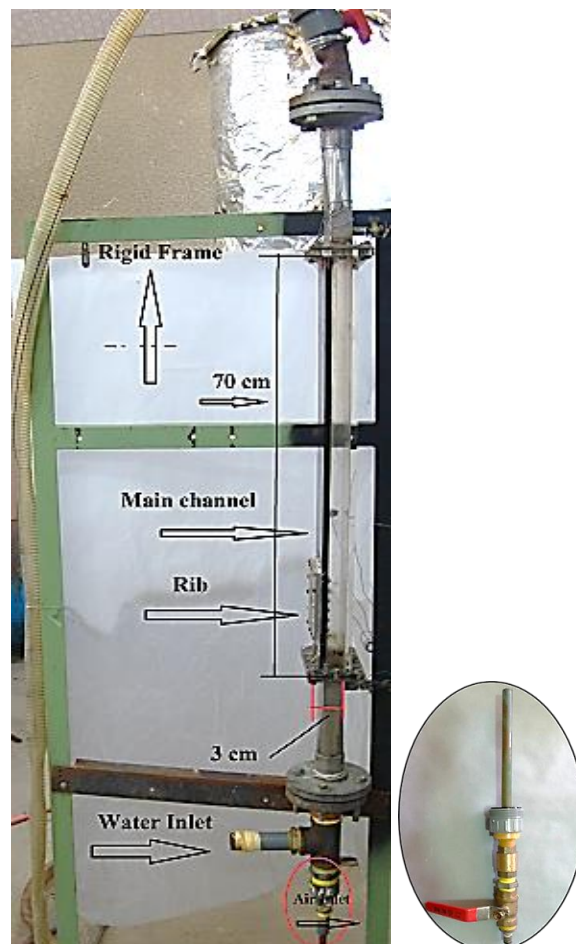


Fig. 2. The test rig viewd



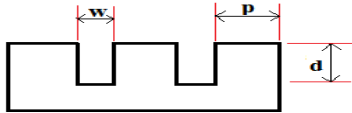
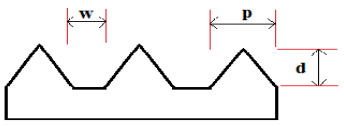
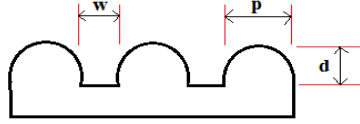
Semi-Circle Rib

Rectangular Rib

Triangular Rib

Fig. 3. Photos of the three type of ribs

Table 1
 Dimensions of the three types of ribs

Case No.	Dimensions in (cm)			Ribs
	w	P	d	
1	0.5	1.2	0.6	
2	0.5	1.2	0.6	
3	0.5	1.2	0.6	

2.1 Experimental Calculations

Superficial velocities were obtained for air and water and utilized in the graphs for showing the influence of raising it upon pressure drop results. The rate of flow was measured straightforward from the flowmeter and employed for calculating the superficial velocity by Eq. (1) [3-4].

$$U = \frac{Q}{A} \tag{1}$$

Re no. can be obtained by Eq. (2)

$$Re = \frac{\rho U D_h}{\mu} \tag{2}$$

Where,

$$D_h = \frac{4A}{W} \tag{3}$$

3. Numerical Solution

Computational fluid dynamic is used for problem analyzing using algorithms as well as numerical analysis via the physical domain division into many cells having a tiny scale and solving the governing equations for every cell, Oleiwi [18]. Ansys Fluent (15.0) was employed for studying the two phase-flow characteristics utilizing a smooth channel with ribs. Mixture model was set for the simulations of two-phase flow. Liquid water and air were set as the two-phase flow, Table 2 shows the two fluid

properties as have been set by fluent database. The superficial velocities effect of air and water and shapes of ribs on the pressure drop for both smooth and ribbed channel were studied. Modeled of the geometry of the system was done like a two-dimensional structure for the flow having two phases with a vertical dimension of 70 cm and a horizontal dimension of 3 cm. The rectangular channel geometry was separated into tiny quadrilateral elements (grid having a quadrilateral structure) utilizing the combined meshing. Values for the under-relaxation factor used for the two-phase flow are shown in Table 3. Mesh size was set as 0.002 m for all the channel, the number of elements and nodes were (7306, 7330, and 7381) and (7891, 7925, and 7966) for (semi-circular, rectangular, and triangular) respectively. Figure 4 depicts the smooth and channel mesh having 3 kinds of ribs. The value of γ^+ for all the computations were kept less than 75 at the wall surface.

Table 2
 Fluid Properties

Property	Water – Liquid (Ansys Fluent 15.0 Database)	Air – Gas (Ansys Fluent 15.0 Database)
Density (kg/m ³)	998.2	1.225
Thermal conductivity (W/m.K)	0.6	0.0242
Viscosity (kg/m.s)	0.001003	1.7894e-05

Table 3
 Under Relaxation Factor

Variable	Relaxation factors Two phases (Water-Air)
Pressure	0.3
Momentum	0.5
Volume fraction	0.5
Energy	0.8

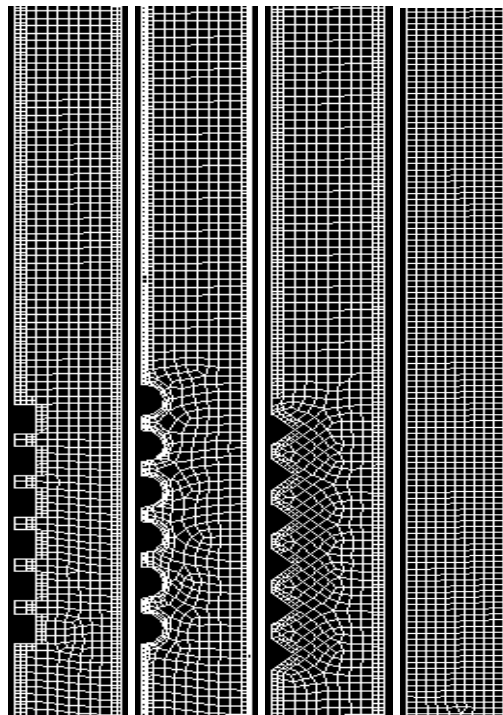


Fig. 4. The mesh of smooth and ribbed channel

For simulating the model of two-phase flow, the subsequent assumptions were done: Turbulent flow, transient flow, incompressible flow, pressure-based solver, and 2D zone, also the gravity in “Y” direction was (-9.81) m.s⁻². The time set was set as 1 with 4 number of time steps, the maximum iteration for each time set was set as 200, Figure 5 shows the residuals for one of the tests that was performed. The continuity conservation and momentum equations were solved for every phase by a blend model; this model was employed, where phases travel with various velocities. The continuity equation was employed for calculating the volume fraction of the phase. Therefore, the primary and secondary phases volume fractions for a control volume can be any value within the range (0 - 1) (Fluent User’s Guide, 2006; Habeeb and Al-Turaihi, 2013), based upon the space that is occupied via the primary and secondary phases. The governing equations solved by Ansys fluent are as follows.

The continuity equation represented by Eq. (4).

$$\frac{\partial}{\partial t}(\rho_m) + \nabla \cdot (\rho_m \vec{v}_m) = 0 \tag{4}$$

Where,

\vec{v}_m : Mass-averaged velocity and can be written in this form:

$$\vec{v}_m = \frac{\sum_{k=1}^n \alpha_k \rho_k \vec{v}_k}{\rho_m} \tag{5}$$

ρ_m : Mixture density

$$\rho_m = \sum_{k=1}^n \alpha_k \rho_k \tag{6}$$

α_k : Phase (k) volume fraction

Equation of momentum represented by Eq. (7).

The general shape of such eq. is given as:

$$\frac{\partial}{\partial t}(\rho_m \vec{v}_m) + \nabla \cdot (\rho_m \vec{v}_m \vec{v}_m) = -\nabla P + \nabla \cdot [\mu_m (\nabla \vec{v}_m + \nabla \vec{v}_m^T)] + \rho_m \vec{g} + \vec{F} + \nabla \cdot \left(\sum_{k=1}^n \alpha_k \rho_k \vec{v}_{dr,k} \vec{v}_{dr,k} \right) \tag{7}$$

Where:

n : Phases number

\vec{F} : Body force

μ_m : Viscosity of mixture that is given as:

$$\mu_m = \sum_{k=1}^n \alpha_k \mu_k \tag{8}$$

Where, $\vec{u}_{dr,k}$: Velocity of drift for the secondary phase (k), and

$$\vec{u}_{dr,k} = \vec{u}_k - \vec{u}_m \tag{9}$$

The utilized boundary conditions for such model include the superficial velocity of water, the superficial velocity of air, and the pressure of outlet.

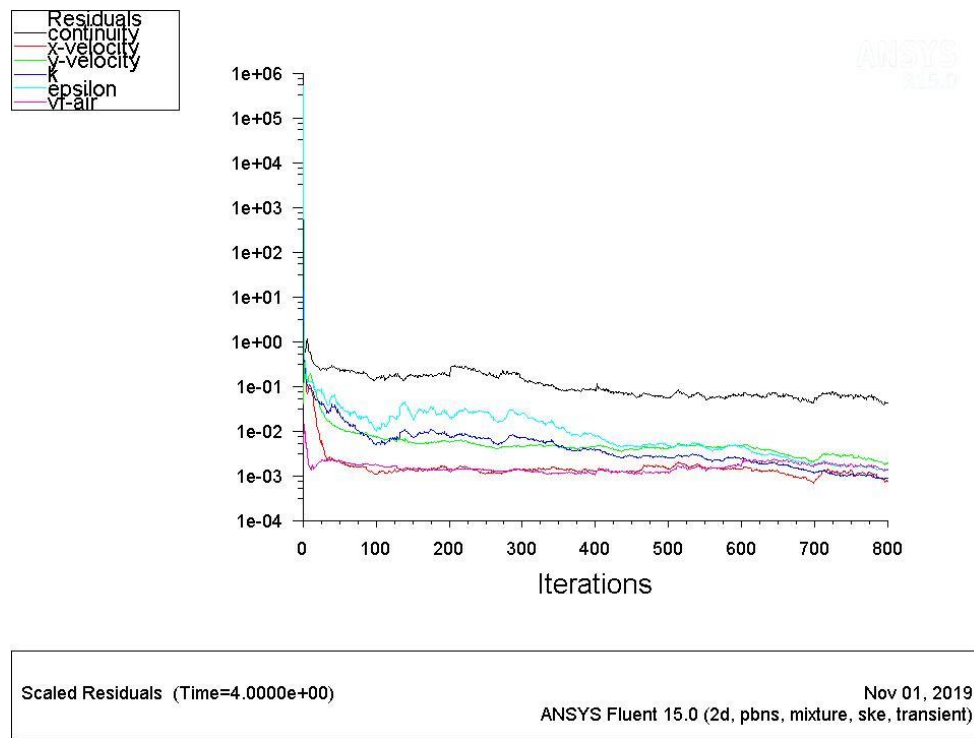


Fig. 5. Residuals for one of the performed tests

3.1 Turbulent Model Equations

The turbulent model used for this computational study is k-epsilon with RNG mixture model. The general equations for this model is as (10-11).

$$\frac{\partial}{\partial t}(\rho_m k) + \nabla \cdot (\rho_m \vec{v}_m k) = \nabla \cdot \left(\frac{\mu_{t,m}}{\sigma k} \nabla k \right) + G_{k,m} - \rho_m \epsilon \tag{10}$$

$$\frac{\partial}{\partial t}(\rho_m \epsilon) + \nabla \cdot (\rho_m \vec{v}_m \epsilon) = \nabla \cdot \left(\frac{\mu_{t,m}}{\sigma_\epsilon} \nabla \epsilon \right) + \frac{\epsilon}{k} (C_{1\epsilon} G_{k,m} - C_{2\epsilon} \rho_m \epsilon) \tag{11}$$

where

C: Constant

k: Momentum exchange coefficient

ϵ : Turbulent dissipation rate (m^2/s^3)

σ : Surface tension (kg/m)

3.2 Boundary and Operating Conditions

The bottom edge of the two-dimensional duct was set as an inlet velocity, the edge for the two-dimensional model was splits into a number of small edges were the water and air enter the duct respectively through these edges. The velocity of the water and air was changed a number of times to have a different range of results from the tests. The outlet edge was set as an outlet pressure. The surface body of the two-dimensional model was set as fluid which was occupied by water and air. Table 4 shows the

Table 4
Boundary Conditions

Zone	Boundary Type
	Two phases (Water-Air)
Channel inlet W	Water superficial velocity
Channel inlet A	Air superficial velocity
Channel outlet	Outlet pressure
Channel content	Water – Air

3.3 Mesh Validation

The type of mesh used for all the simulations are the same, which is Quadrilateral mesh. Changing in the geometry of duct by adding ribs would change the number of element and nodes for the mesh. Mesh element size was validated by choosing three sizes for comparison. 0.5 mm, 2 mm, 5 mm and was tested for a number of water and air flow rates. At 9 L/min water flow rate and 600 L/hr air flow rate in Figure 6 the volume fraction of water was shown for the three number of mesh sizes that were tested. From Figure 6 it clear that 2 mm element size is the best one among the tested sizes, the other element sizes did not give a good results for the flow around the ribs, also Using small size mesh will increase the simulation time for each test.

4. Results and Discussions

The results of the experimental and numerical works are for the flow with two phases into a channel having a rectangular, semi-circular, and triangular shape ribs. Comparison between the results of the experimental and the numerical works was made for studying and investigating the two-phase flow, and comparison among the numerical data of the smooth and ribbed channel was made in order to show the effect of adding ribs upon drop of pressure. The influence of increasing water superficial velocity within (0.0333-0.0888 m/s), air superficial velocity within (0.0555-0.1666 m/s), and effect of the ribs shape on the pressure distribution were obtained. Figures 7 to 11 show the increasing of the water superficial velocity effect upon pressure drop results with different shapes of ribs (triangular, semi-circle, and rectangular) for various values of superficial velocity of air. These figures depict the drop of pressure increase when the flow of air increases at the specific flow of water. In Figure 7 for water flow rate of 6 L/min and air flow rate of 1800 L/hr, the triangular shaped ribbed duct has a pressure difference of 11.1 kpa. While for the same water and air flow rates the rectangular shape ribbed duct have a pressure difference of 10.7 kpa, and the semi-circular shape ribbed duct have a pressure difference of 10.6. The semi-circular rib is the finest shape for decrease pressure difference whereas the triangular ribs increasing the pressure difference. Due to the effect of leading and trailing edges of the ribs. Thus, the triangular rib had a higher rate of pressure difference 11.1 kpa than the other ribs (10.7, and 10.6 kpa), since it possessed the smallest tip and a

sharp edge. so the area of the leading edge and the trailing edge behavior were at, low magnitude for the ribs having a triangular shape, and high magnitude the other ribs having a semi-circular and rectangular shape. This provided additional area for pressure drop and generated a turbulence flow higher. The pressure difference for triangular shape ribbed duct at 14 L/min water flow rate and 900 L/hr air flow rate were 11 kpa while at the same flow rates the other two ribbed ducts have a pressure difference of 10.3 kpa and 10.5 kpa for rectangular and semi-circular ribbed ducts respectively, Figure 10. Figures 12 and 13 show the effect of water flow rate at specific airflow rate for the three types of ribbed that were investigated. When the water and air superficial velocity raised, the flow turbulence in channel increased, as shown in figures. Figures 14, 15 and 19 reveal the behavior of the experimental flow by the photographs obtained for the test channel and visually compared with the obtained contour for the water volume fraction via the simulation numerically. The channel with a rectangular shape was equipped with a rib having a triangular shape, where a turbulence flow generated higher than the other shapes of ribs, because it had a sharper edge than the other edges for the semi-circle and rectangular ribs, and this provides more area between the adjacent ribs. An adjacent likeness for the behavior of flow between experimental photographs and the images of water volume fraction was obtained by ANSYS (Fluent 15.0). Figure 15 represents the average difference of pressure with specific discharge of water for the various values of discharge of air for a semi-circular rip. If the discharge of water or air rises, the average difference of pressure will rise. This is owing to the increment of the discharge of water or air that results in velocity increments. Already, it's observed that the average difference of pressure possesses an important effect upon the behavior of the two phases flow. So, it's anticipated that the instability of flow will also rely the difference of. Figures 16 and 18 demonstrate the contours of velocity vector distribution for the semi-circular rip and three types of rip used experimentally and numerically. Each figure is for specific magnitudes of the superficial velocity of water with a different value of the superficial velocity of air. These figures show that the amplitude appeared at a specific position, where the ribs positioned. Figure 20 illustrate closer look for a single rib in the duct for the three types of ribs (triangular, rectangular, and semi-circular) for the same water and air flow rates 11 L/min, and 600 L/hr, respectively.

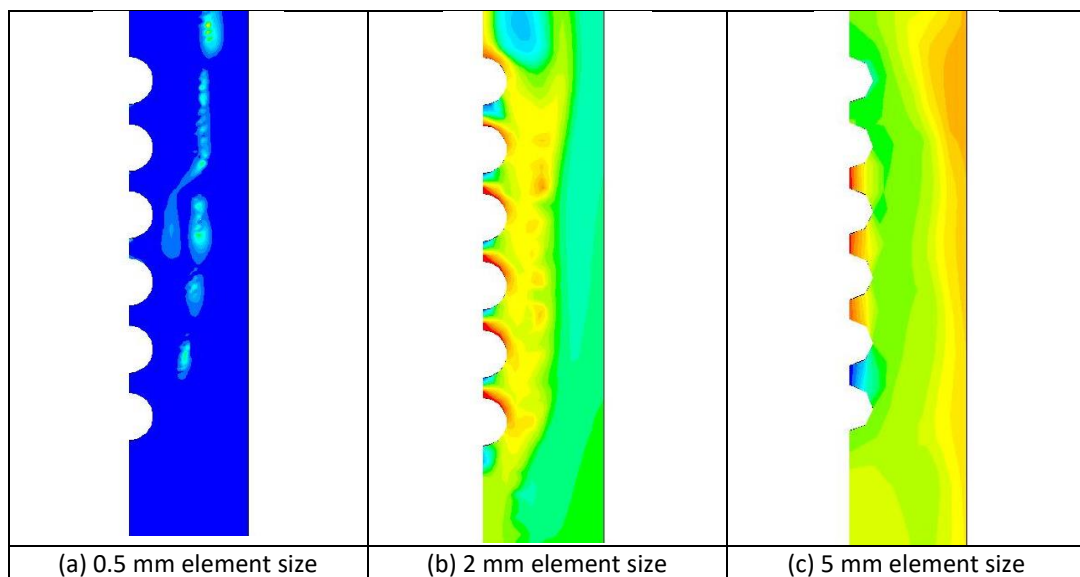


Fig. 6. Mesh validation test

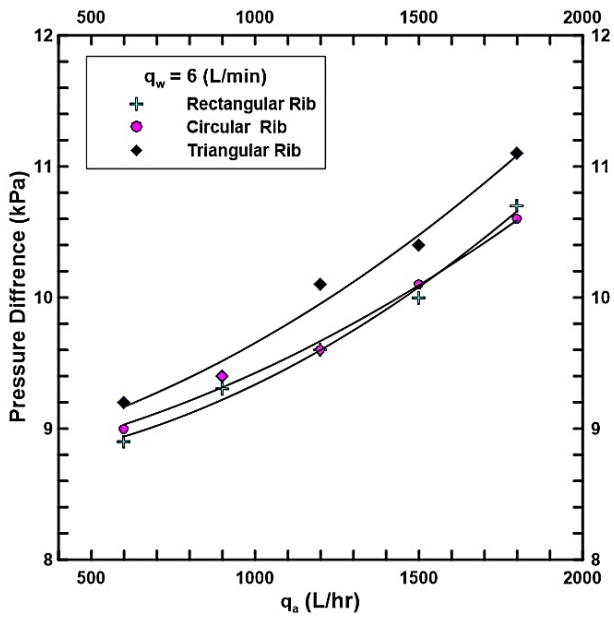


Fig. 7. Influence of the rib shape upon the drop of pressure with the variable air flow rate and constant water flow rate

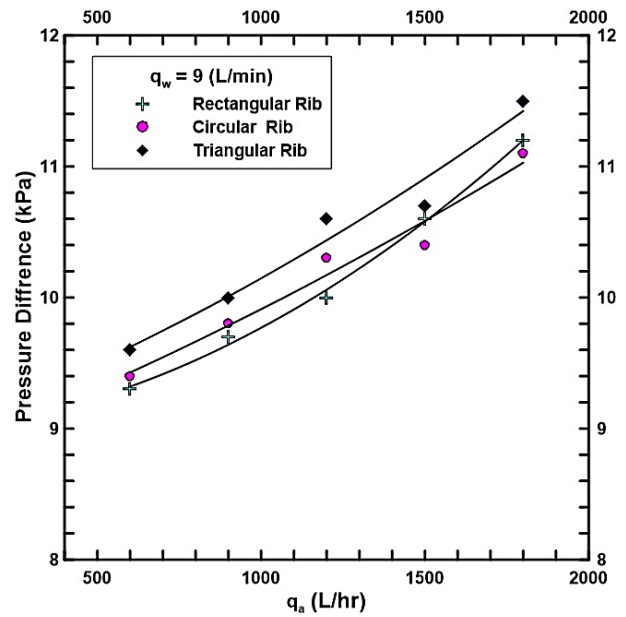


Fig. 8. Influence of the rib shape upon the drop of pressure with the variable air flow rate and constant water flow rate

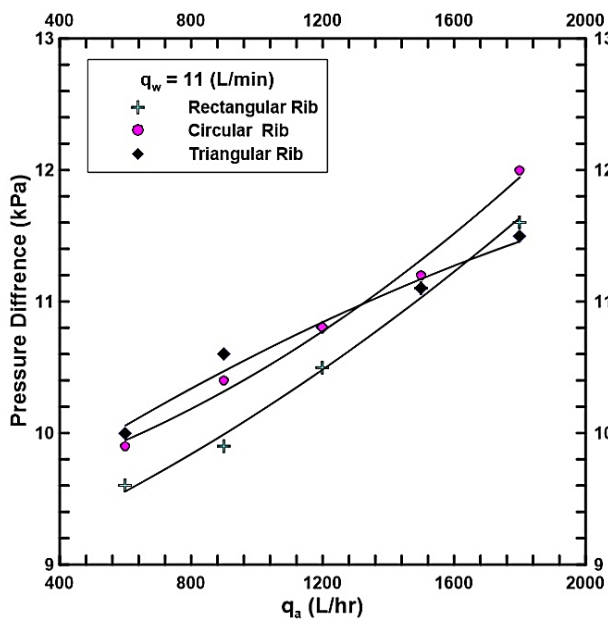


Fig. 9. Influence of the rib shape upon the drop of pressure with the variable air flow rate and constant water flow rate

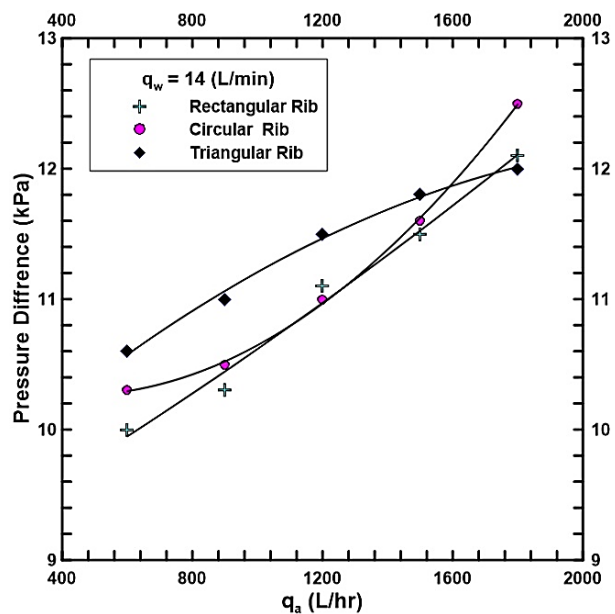


Fig. 10. Influence of the rib shape upon the drop of pressure with variable air flow rate and constant water flow rate

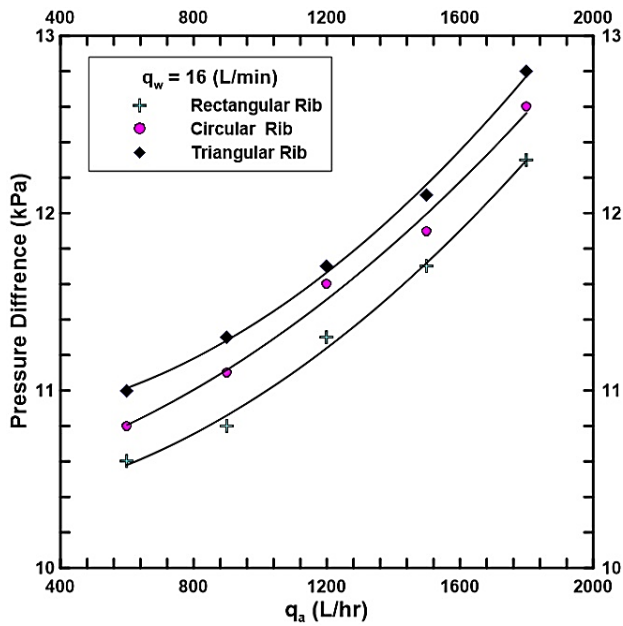


Fig. 11. Influence of the rib shape upon the drop of pressure with the variable air flow rate and constant water flow rate

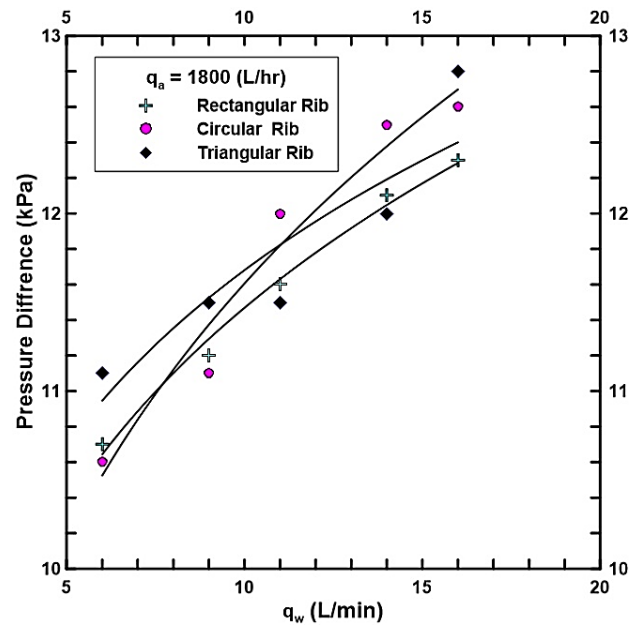


Fig. 12. Influence of the rib shape upon the drop of pressure with the variable air flow rate and constant water flow rate

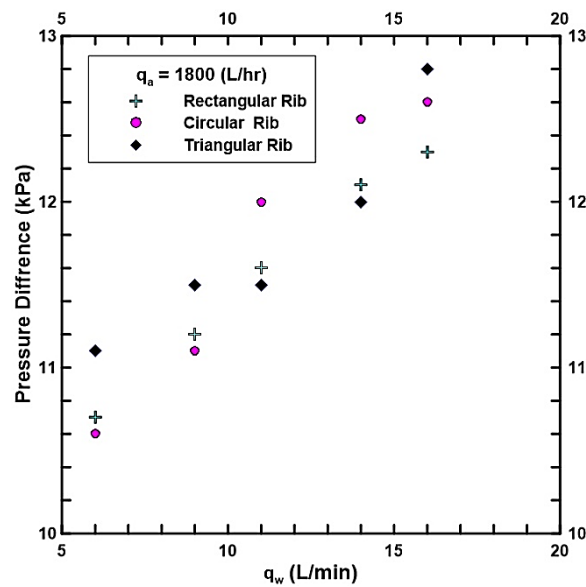


Fig. 13. Influence of the rib shape upon the drop of pressure with the variable water flow rate and constant air flow rate

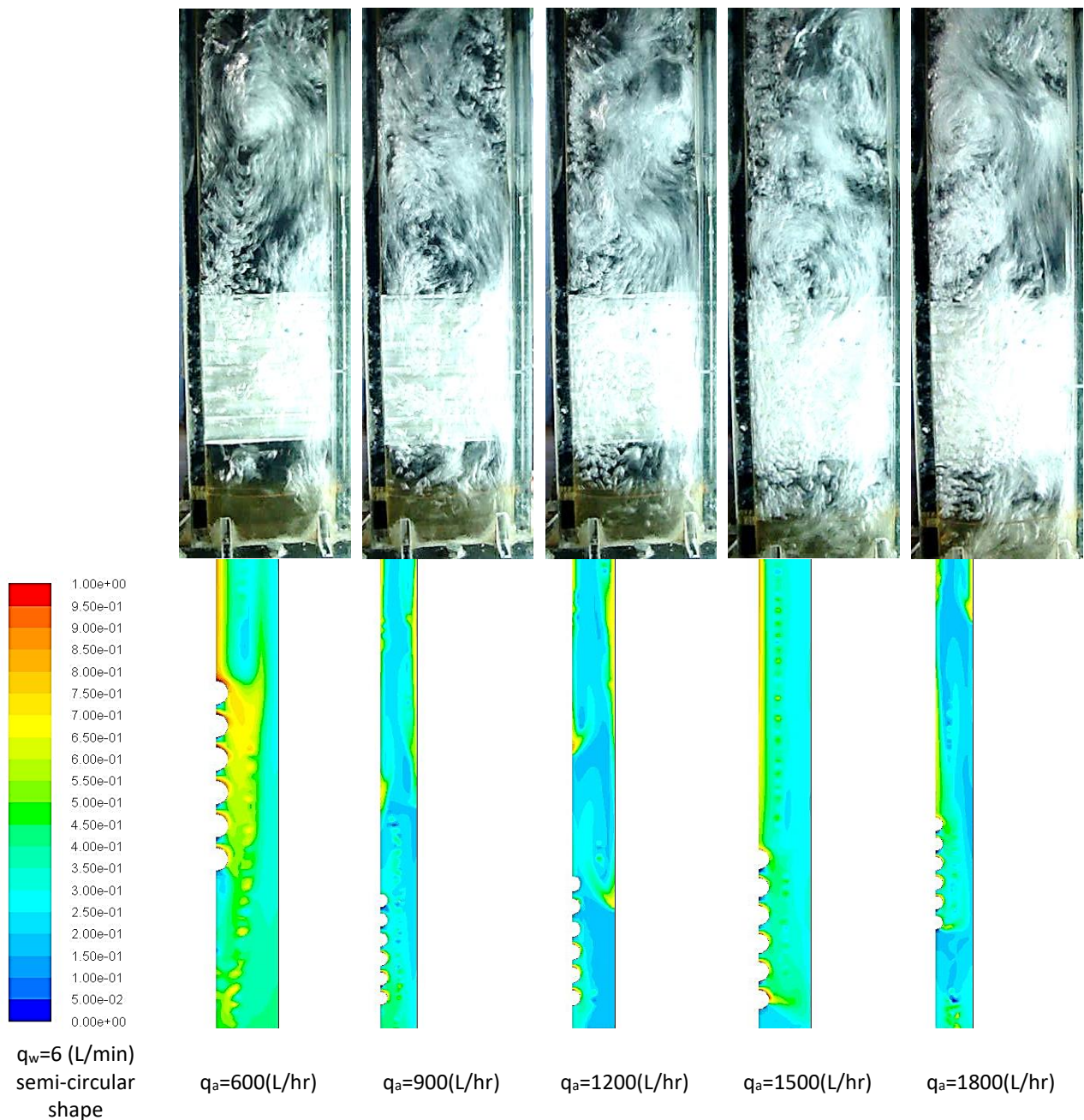


Fig. 14. Effect of semi-circular rib shape on the volume fraction with the air flow rate and constant water flow rate

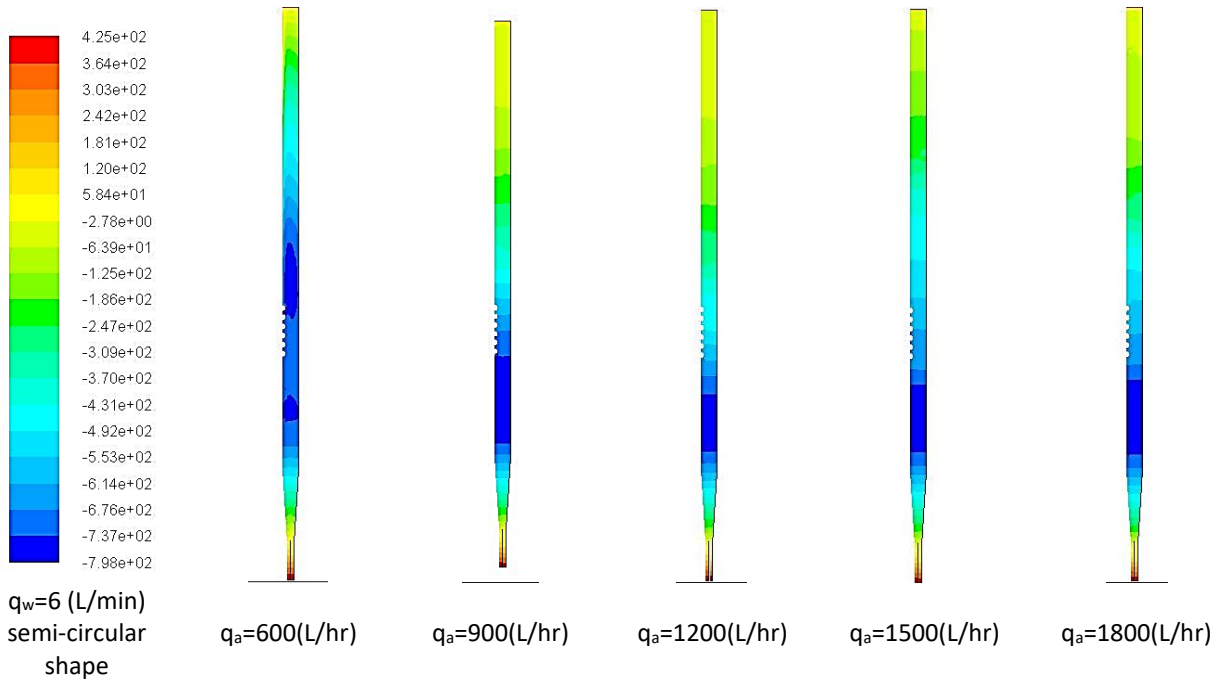


Fig. 15. Influence of the semi-circular rib shape upon the drop of pressure with the variable air flow rate and constant water flow rate

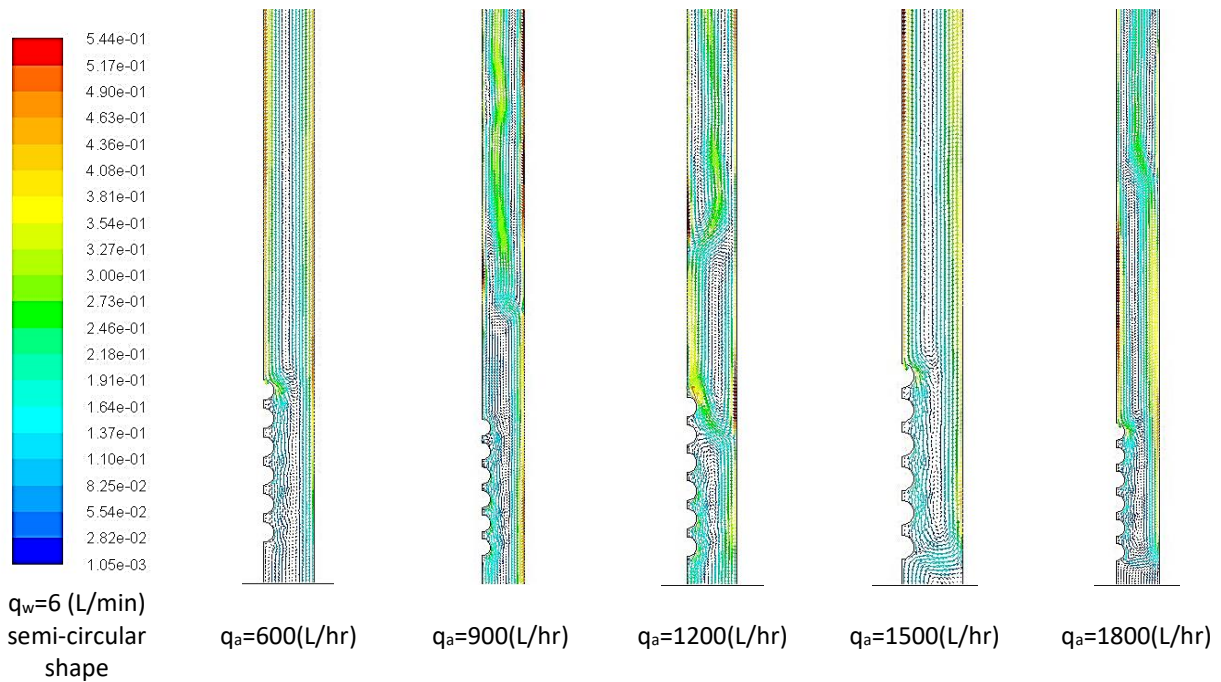


Fig. 16. Effect of semi-circular rib shape on the velocity vector with the variable air flow rate and constant water flow rate

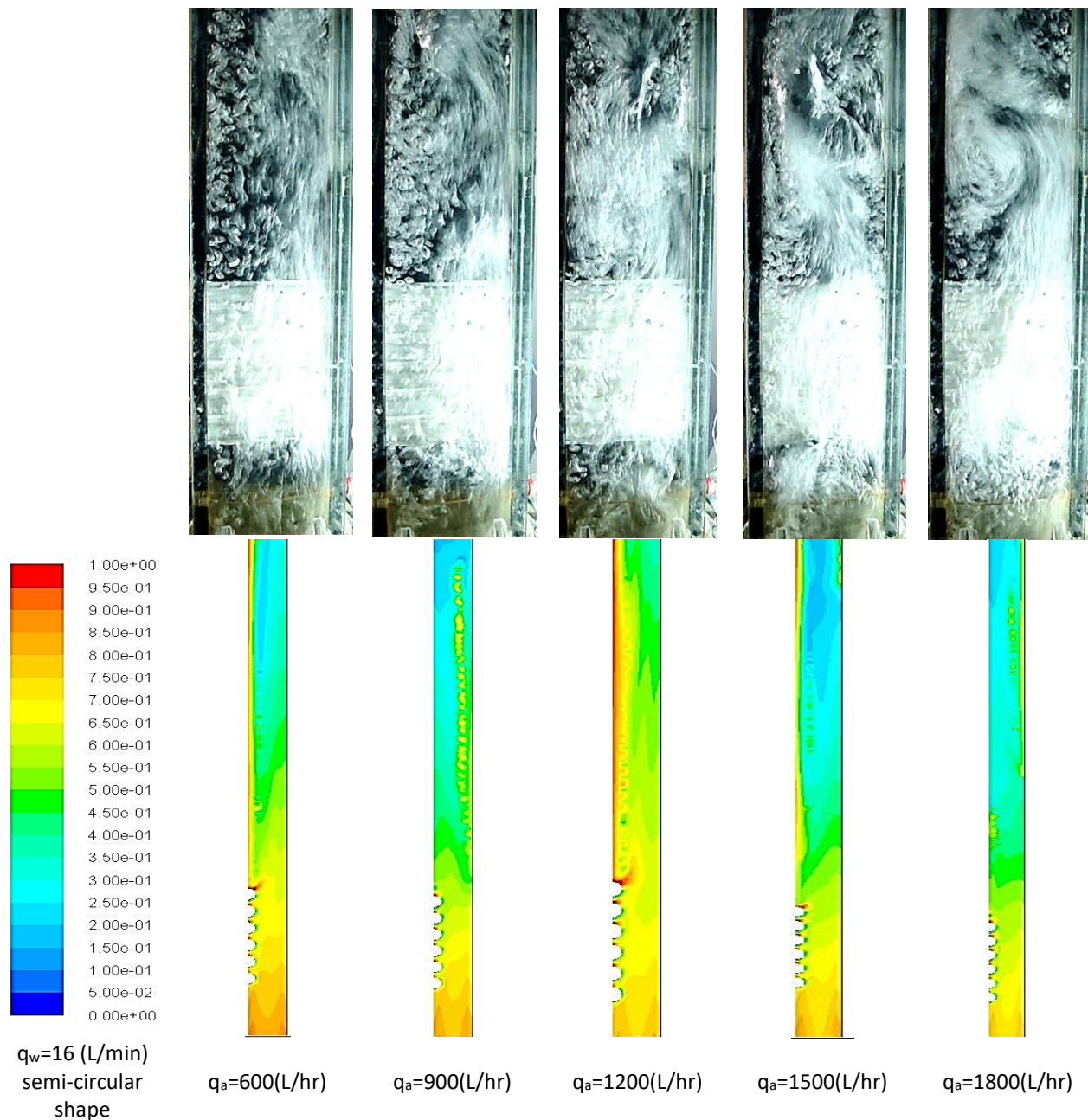


Fig. 17. Effect of semi-circular rib shape on the volume fraction with the variable air flow rate and constant water flow rate

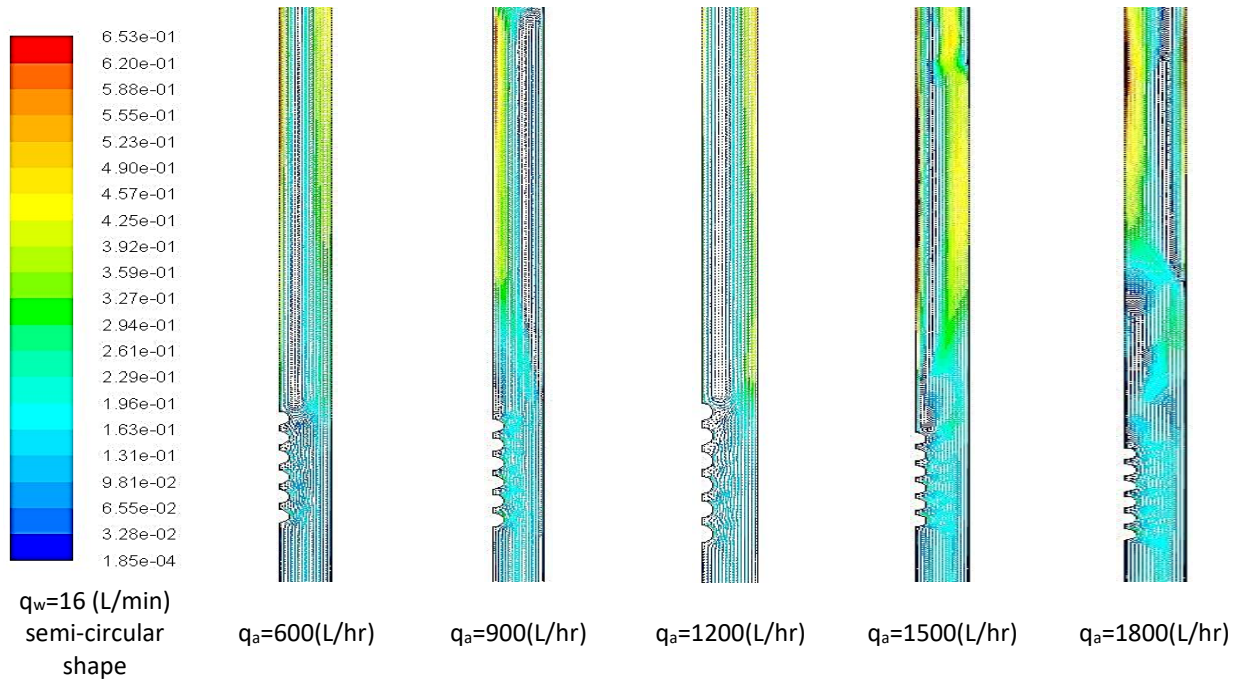
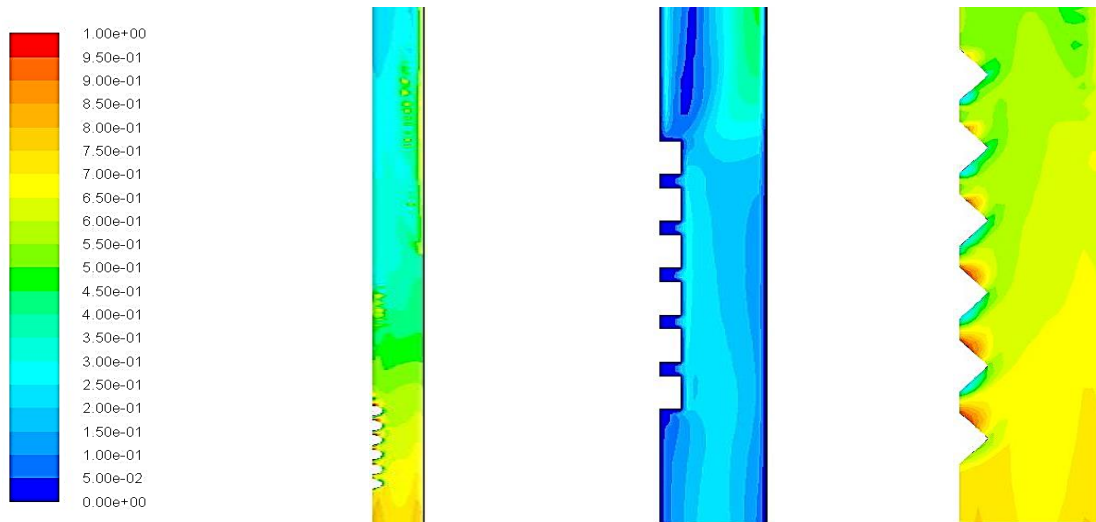


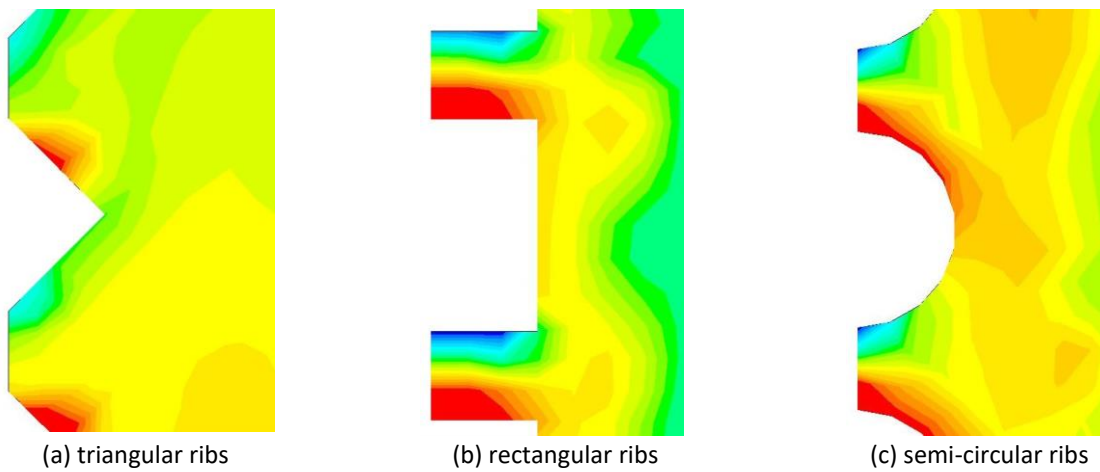
Fig. 18. Effect of semi-circular rib shape on the velocity vector with the variable air flow rate and constant water flow rate





$q_w = 6$ (L/min), $q_a = 1800$ (L/hr) for semi-circular, rectangular and triangular shape

Fig. 19. Effect of different rib shape on the volume fraction with the variable air flow rate and constant water flow rate

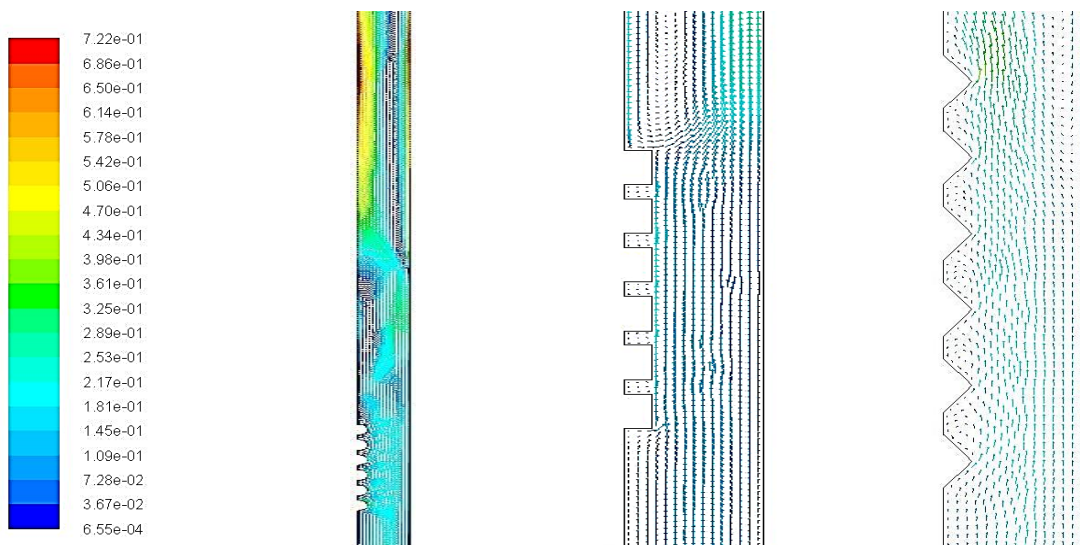


(a) triangular ribs

(b) rectangular ribs

(c) semi-circular ribs

Fig. 20. comparison between the three types of ribs



$q_w = 6$ (L/min), $q_a = 1800$ (L/hr) for semi-circular, rectangular and triangular shape

Fig. 21. Effect of different rib shape on the velocity vector with the variable air flow rate and constant water flow rate

4. Conclusions

This investigation has concentrated on the phase spreads in less quality scatter two phases flows around an obstacle. It composes of a theoretical work having a high general nature and an experimental work that highlights the bubbly flows around a cylinder in a horizontal channel. The summarized concluding remarks are as follows:

- i. Random-like way, creating pressure, velocity and fluctuations of the phase fraction: the flow is not steady, even if the liquid and gas flow rates are maintained fixed at the inlet of the channel.
- ii. The sensor of pressure at the outlet and inlet of the section of test recorded the pressures that fluctuate with the time owing to the two-phase influence. In addition, if the discharge of water or air rises, the average difference of pressure will rise.
- iii. Owing to the vigorous variations of the value and the local discharges direction of the flow of fluid and the difference of density between the fluid and the scattered phase, the distribution pattern of the local phase varies noticeably around the obstacle.

It has to be noticed that the bubble size prediction does not rightly characterize the noted size in the experiments. That is owing to discrepancy in the numerical description of the vapor bubble as well as the visual bubble boundary.

Acknowledgement

Laith Jaafer Habeeb and Hasan Shakir Majdi would like to thank University of Technology / Training and Workshop Center, Baghdad – Iraq and Al-Mustaqbal University College / Chemical and petroleum industries engineering department, Babil – Iraq for its support in the present work.

Reference

- [1] Weisman, J., J. Lan, and P. Disimile. "Two-phase (air-water) flow patterns and pressure drop in the presence of helical wire ribs." *International journal of multiphase flow* 20, no. 5 (1994): 885-899.
[https://doi.org/10.1016/0301-9322\(94\)90099-X](https://doi.org/10.1016/0301-9322(94)90099-X)
- [2] Gao, Xiufang, and Bengt Sundén. "Heat transfer and pressure drop measurements in rib-roughened rectangular ducts." *Experimental Thermal and Fluid Science* 24, no. 1-2 (2001): 25-34.
[https://doi.org/10.1016/S0894-1777\(00\)00054-6](https://doi.org/10.1016/S0894-1777(00)00054-6)
- [3] Asano, Hitoshi, Nobuyuki Takenaka, and Terushige Fujii. "Flow characteristics of gas–liquid two-phase flow in plate heat exchanger:(Visualization and void fraction measurement by neutron radiography)." *Experimental Thermal and Fluid Science* 28, no. 2-3 (2004): 223-230.
[https://doi.org/10.1016/S0894-1777\(03\)00043-8](https://doi.org/10.1016/S0894-1777(03)00043-8)
- [4] Ansari, M. R., and B. Arzandi. "Two-phase gas–liquid flow regimes for smooth and ribbed rectangular ducts." *International Journal of Multiphase Flow* 38, no. 1 (2012): 118-125.
<https://doi.org/10.1016/j.ijmultiphaseflow.2011.08.008>
- [5] Habeeb, Laith Jaafer, and Riyadh S. Al-Turaihi. "Experimental Study and CFD Simulation of Two-Phase Flow around Triangular Obstacle in Enlarging Channel." *Int. J. Eng. Res. Appl* 3, no. 4 (2013): 2036-2042.
- [6] Jiang, Guangwen, Xiaojun Shi, Guanwen Chen, and Jianmin Gao. "Study on flow and heat transfer characteristics of the mist/steam two-phase flow in rectangular channels with 60 deg. ribs." *International Journal of Heat and Mass Transfer* 120 (2018): 1101-1117.
<https://doi.org/10.1016/j.ijheatmasstransfer.2017.12.082>
- [7] Parsaiemehr, Mohammad, Farzad Pourfattah, Omid Ali Akbari, Davood Toghraie, and Ghanbarali Sheikhzadeh. "Turbulent flow and heat transfer of Water/Al₂O₃ nanofluid inside a rectangular ribbed channel." *Physica E: Low-Dimensional Systems and Nanostructures* 96 (2018): 73-84.
<https://doi.org/10.1016/j.physe.2017.10.012>
- [8] Jiang, Guangwen, Jianmin Gao, Xiaojun Shi, Wang Zhao, and Yunlong Li. "Flow and Heat Transfer of Mist/Steam Two-Phase Flow in Two-Pass Rectangular Channels With Paralleled and V-Shaped Rib Turbulators." In *ASME 2018 International Mechanical Engineering Congress and Exposition*. American Society of Mechanical Engineers Digital Collection, 2018.

- <https://doi.org/10.1115/IMECE2018-88532>
- [9] Shi, Xiaojun, Guangwen Jiang, Jianmin Gao, Guanwen Chen, and Liang Xu. "Heat transfer comparison investigation of mist/steam two-phase flow and steam in a square smooth channel." *Proceedings of the Institution of Mechanical Engineers, Part A: Journal of Power and Energy* 233, no. 7 (2019): 877-889.
<https://doi.org/10.1177/0957650919839593>
- [10] Ayagara, Aravind Rajan, André Langlet, and Ridha Hambli. "On dynamic behavior of bone: experimental and numerical study of porcine ribs subjected to impact loads in dynamic three-point bending tests." *Journal of the mechanical behavior of biomedical materials* 98 (2019): 336-347.
<https://doi.org/10.1016/j.jmbbm.2019.05.031>
- [11] Park, Jin Ho, Hyun Sun Park, and Mooneon Lee. "Experimental study on evaluation of effective diameter for non-spherical particles in predicting pressure gradients of water/air two-phase flow in particle beds." *International Journal of Heat and Mass Transfer* 140 (2019): 139-146.
<https://doi.org/10.1016/j.ijheatmasstransfer.2019.05.072>
- [12] Wang, Yubo, Zhigang Liu, Yingjie Chang, Xiangyuan Zhao, and Liejin Guo. "Experimental study of gas-liquid two-phase wavy stratified flow in horizontal pipe at high pressure." *International Journal of Heat and Mass Transfer* 143 (2019): 118537.
<https://doi.org/10.1016/j.ijheatmasstransfer.2019.118537>
- [13] Jawad, Layth H., Shahrir Abdullah, Rozli Zulkifli, and Wan Mohd Faizal Wan Mahmood. "Numerical Investigation on the Effect of Impeller Trimming on the Performance of a Modified Compressor." *CFD Letters* 5, no. 4 (2013): 174-184.
- [14] <https://www.hitachi.com>
- [15] <https://www.worthington-creyssensac.com>
- [16] www.qf-meter.com
- [17] www.sony.co.uk
- [18] Sarah H. Oleiwi. "Experimental and Numerical Investigation of Multi-phase Flow in Fluidized Bed Column." MSc Thesis, College of Engineering, University of Babylon, 2016.